

Angular and chiral content of the ρ and ρ' mesons

C. Rohrhofer*

Institut für Physik, FB Theoretische Physik, Universität Graz

E-mail: christian.rohrhofer@uni-graz.at

M. Pak

Institut für Physik, FB Theoretische Physik, Universität Graz

E-mail: markus.pak@uni-graz.at

L. Ya. Glozman

Institut für Physik, FB Theoretische Physik, Universität Graz

E-mail: leonid.glozman@uni-graz.at

We identify the chiral and angular momentum content of the leading quark-antiquark Fock component for the $\rho(770)$ and $\rho(1450)$ mesons using a two-flavor lattice simulation with dynamical Overlap Dirac fermions. We extract this information from the overlap factors of two interpolating fields with different chiral structure. We find that in the angular momentum basis the $\rho(770)$ is a 3S_1 state, in accordance with the quark model. The $\rho(1450)$ is a 3D_1 state, showing that the quark model wrongly assumes the $\rho(1450)$ to be a radial excitation of the $\rho(770)$. Further, we apply a low-mode truncation scheme of the Dirac operator and study its effects on the chiral structure of the mesons.

34th annual International Symposium on Lattice Field Theory

24-30 July 2016

University of Southampton, UK

*Speaker.

1. Introduction

The potential constituent quark model has been quite successful in describing the low-lying hadron spectrum [1]. Being an effective classification scheme, it does not care about foundations in terms of underlying QCD dynamics. Despite its successes the non-relativistic description clearly has limitations: especially the role of the $\rho(1450)$ and $\rho(1700)$ mesons is not very clear.

In this paper we investigate the angular momentum content of the $\rho(770)$, $\rho(1450)$ and $\rho(1700)$ mesons. In the spectroscopic notation $n^{2S+1}l_J$ the $\rho(770)$ is assigned to the 1^3S_1 state by the quark model. The $\rho(1450)$ is assigned to the 2^3S_1 state, hence being the first radial excitation of the $\rho(770)$. The $\rho(1700)$ is assigned to the 1^3D_1 state. However, this assumption is by far not clear from the underlying QCD dynamics, and is an output of the non-relativistic potential description of a meson as a two-body system.

For identifying the angular momentum content of the leading quark-antiquark Fock components by a lattice simulation we make use of the chiral-parity group [3, 4, 5]. The crucial ingredients to such a study are the overlap factors obtained with operators that form a complete set with respect to the chiral-parity group. From these overlap factors the chiral content of a state can be identified. Then, given a unitary transformation between the chiral basis and the $^{2S+1}l_J$ basis we can reconstruct the angular momentum content. Since the chiral content is important for such a study we need a lattice fermion discretization, which respects chiral symmetry. This is why we use overlap fermions, which distinguishes the present study from the previous ones.

Further, we remove the low-lying Dirac eigenmodes of the spectrum, which has been done recently to show an emergent $SU(2N_f)$ symmetry in the QCD spectrum. This symmetry connects all flavors and quark chiralities, which means in the two-flavor case that u_L, u_R, d_L, d_R are connected with each other. Here we study the effect of the Dirac eigenmode removal on the chiral classification of the mesons.

The main study is presented in detail in Ref. [2].

2. Formalism

To generate states with ρ quantum numbers $I = 1$ and $J^{PC} = 1^{--}$ two different local interpolators can be used, which belong to two distinct chiral representations

$$J_\rho^V(x) = \bar{\Psi}(x)(\tau^a \otimes \gamma^j)\Psi(x) \quad \in (0, 1) \oplus (1, 0) \quad (2.1)$$

$$J_\rho^T(x) = \bar{\Psi}(x)(\tau^a \otimes \gamma^0 \gamma^j)\Psi(x) \quad \in (1/2, 1/2)_b. \quad (2.2)$$

We denote them according to their Dirac structure as *vector* (V) and *pseudotensor* (T) interpolators. The interpolators (2.1), (2.2) transform differently under $SU(2)_L \times SU(2)_R$ and therefore belong to two different chiral representations. If chiral symmetry would be manifest in nature, these two interpolators would generate two different particles. In the real world, where chiral symmetry is broken, a physical ρ -meson is a mixture of two possible chiral representations and consequently both interpolators create the same physical ρ -meson.

In a next step we connect the chiral basis to the angular momentum basis with quantum numbers isospin I and $^{2S+1}l_J$. For spin-1 isovector mesons there are only two allowed states $|1; ^3S_1\rangle$ and

$|1;^3D_1\rangle$, which are connected to the chiral basis by a unitary transformation [6]:

$$|\rho_{(0,1)\oplus(1,0)}\rangle = \sqrt{\frac{2}{3}}|1;^3S_1\rangle + \sqrt{\frac{1}{3}}|1;^3D_1\rangle, \quad (2.3)$$

$$|\rho_{(1/2,1/2)_b}\rangle = \sqrt{\frac{1}{3}}|1;^3S_1\rangle - \sqrt{\frac{2}{3}}|1;^3D_1\rangle. \quad (2.4)$$

We emphasize that the operators (2.1),(2.2) form a complete and orthogonal basis with respect to the chiral group. Given the unitary transformation (2.3),(2.4) they also form a complete and orthogonal basis with respect to the angular momentum content. In order to explore possible different radial behaviour of the $\bar{q}q$ wave functions we supplement the local operators (2.1),(2.2) with different radial smearing levels that make our operator basis physically complete - keeping in mind the leading quark-antiquark component of a meson.

On the lattice we evaluate the correlators $\langle J(t)J^\dagger(0)\rangle$. We apply the variational technique, where different interpolators are used to construct the correlation matrix $\langle J_l(t)J_m^\dagger(0)\rangle = C(t)_{lm}$. By solving the generalized eigenvalue problem

$$C(t)_{lm}u_m^{(n)} = \lambda^{(n)}(t,t_0)C(t_0)_{lm}u_m^{(n)} \quad (2.5)$$

the masses of the states can be extracted in a standard way. Denoting $a_l^{(n)} = \langle 0|J_l|n\rangle$ as the overlap of interpolator J_l with the physical state $|n\rangle$, the relative weight of two interpolators is given by

$$\frac{a_l^{(n)}}{a_k^{(n)}} = \frac{C(t)_{lj}u_j^{(n)}}{C(t)_{kj}u_j^{(n)}}. \quad (2.6)$$

Using vector- and pseudotensor interpolators, we can extract the relative chiral contribution a_V/a_T for each state n . Then via the unitary transformation (2.3),(2.4) we arrive at the angular momentum content of the ρ mesons.

3. Lattice technicalities

3.1 Simulation parameters

We use gauge configurations generously provided by the JLQCD collaboration, see Ref. [7]. The ensemble consists of 100 configurations of two-flavor dynamical Overlap fermions. The topological sector is fixed to $Q_{top} = 0$. Lattice size and spacing are $16^3 \times 32$ at $a \sim 0.12$ fm. The pion mass is at $m_\pi = 289(2)$ MeV [7].

3.2 Resolution scale via smeared sources

The *vector* current J_ρ^V is conserved, i.e. its coupling a_V to the physical state should be independent of the scale. The *pseudotensor* current J_ρ^T is not conserved. Hence, a_T should depend on the scale where it is measured, which makes the ratio a_V/a_T a scale-dependent quantity.

An intrinsic resolution scale is set by the lattice spacing a . If we probe the hadron structure with point-like sources then the result should display a structure of a hadron that is obtained at the scale fixed by the ultraviolet regularization a . In principle we could study the a -dependence by

means of different lattices with different a . However, such a procedure does not allow to measure the structure close to the infrared region, i.e. at large a .

Instead of varying a , we smear the sources of the quark propagators using different widths σ . Clearly, the smeared source cannot supply us with the information about the hadron structure that is sensitive to distances that are smaller than the smearing width σ . Consequently the smearing width σ defines a scale at which we probe the structure of our hadron.

This is done using the Gaussian smearing of the source and sink operators. We use four different smearing widths in this study, whose profiles are plotted in Fig. 1. As definition for the resolution scale we use $R = 2\sigma a$.

The *Super Narrow* source probes the hadron wave function at the resolution ~ 0.25 fm and marks the ultraviolet end of our parameter space. *Narrow* and *Wide* probe the hadron in the mid-momentum region. The *Ultra Wide* source does not resolve details smaller than ~ 0.9 fm and marks our infrared end.

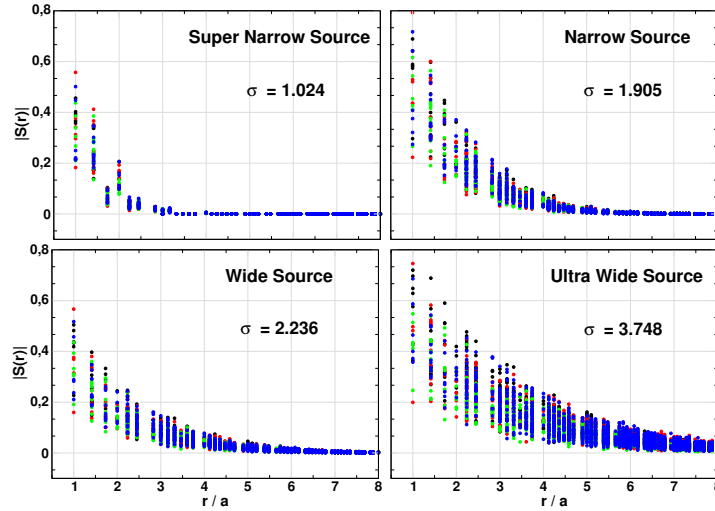


Figure 1: Four different source profiles. Different colors correspond to different gauge configurations.

4. Results

In Fig. 2 we show the lowest eigenvalues of the 8×8 cross-correlation matrix in the full theory ($k = 0$) as well as after truncation of $k = 20$ lowest eigenmodes of the Dirac operator (the issue of truncation will be discussed later on). It can be seen that without truncation the ground state can be reliably extracted, while the effective mass plateau is due to the rather low statistics of poor quality for the first and second excited state. However, after truncation of the lowest 20 modes the signal for these states is greatly improved and we are confident that the poor plateaux for the first and second excited states at $k = 0$ do represent physical states.

To study the ratio a_V/a_T at different resolution scales R we solve the eigenvalue problem (2.5) with operators (2.1) and (2.2) and four different smearings. Then using (2.6) we extract the ratio a_V/a_T as a function of R . In Fig. 3 we show the ratio a_V/a_T at different resolution scales R . Note that there is a clear linear R -dependence on the ratio a_V/a_T for both ρ and ρ' states.

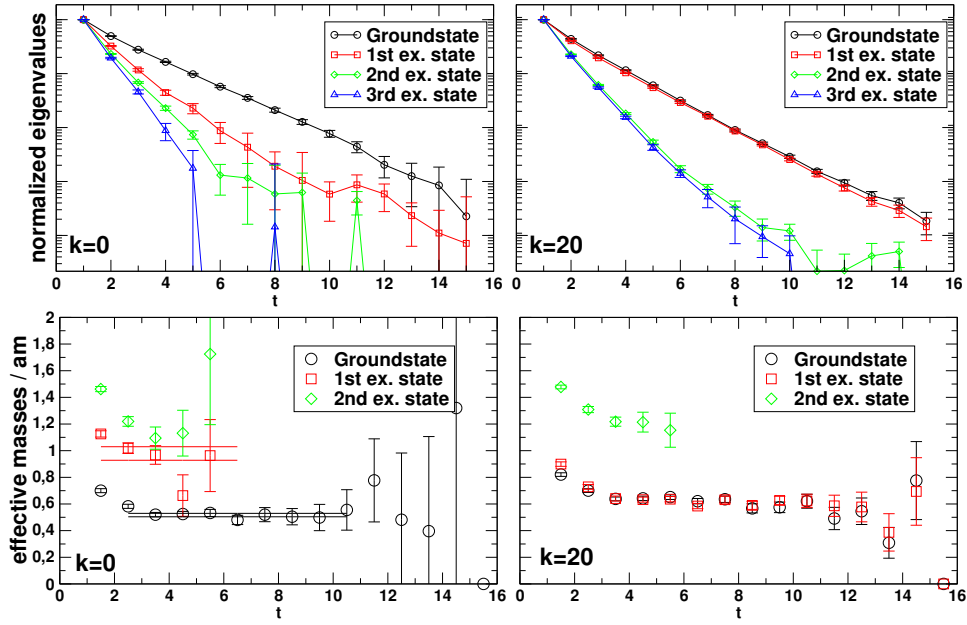


Figure 2: Normalized eigenvalues and effective masses for the full (left) and $k=20$ truncated theory (right).

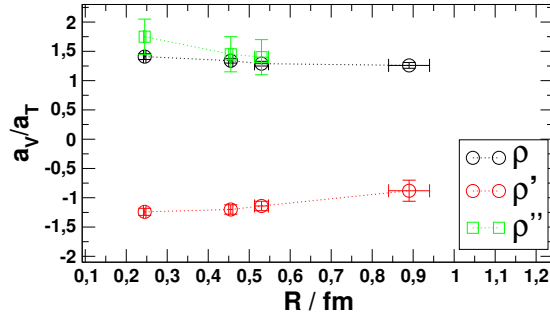


Figure 3: a_V/a_T ratio for different resolutions.

In the infrared, at the resolution scale 0.9 fm, the ratios are given by $a_V/a_T = (1.26 \pm 0.05)$ for the ground state ρ meson, and $a_V/a_T = -(0.88 \pm 0.18)$ for the first excited state. For the second excited state we lose the signal in the infrared and extract the value $a_V/a_T = (1.4 \pm 0.3)$ at 0.53 fm. Using now transformations (2.3),(2.4) we find:

$$|\rho(770)\rangle = + (0.998 \pm 0.002) |^3S_1\rangle - (0.05 \pm 0.025) |^3D_1\rangle, \quad (4.1)$$

$$|\rho(1450)\rangle = - (0.106 \pm 0.09) |^3S_1\rangle - (0.994 \pm 0.005) |^3D_1\rangle. \quad (4.2)$$

$$|\rho(1700)\rangle = + (0.99 \pm 0.01) |^3S_1\rangle - (0.01 \pm 0.12) |^3D_1\rangle. \quad (4.3)$$

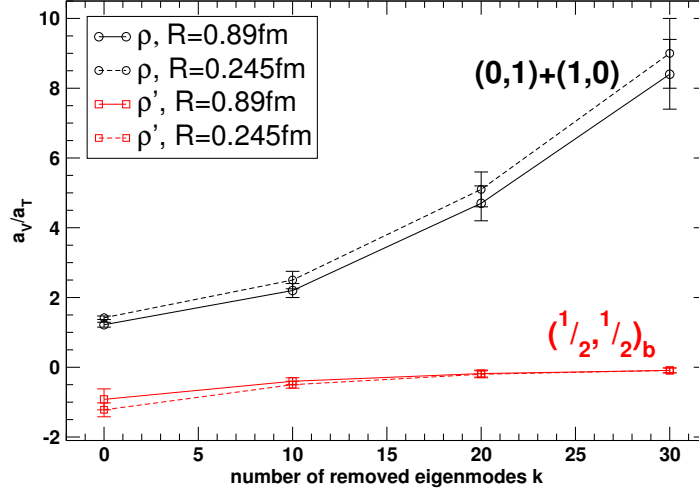


Figure 4: Chiral contributions for a low mode truncated system at $R = 0.89$ fm and $R = 0.245$ fm.

The ground state ρ is therefore practically a pure 3S_1 state, in agreement with the potential quark model assumption. The first excited ρ is, however, a 3D_1 state with a very small admixture of a 3S_1 wave. The second excited state is almost pure 3S_1 state. The latter results are in clear contradiction with the potential constituent quark model that attributes the first excited state of the ρ meson to a radially excited 3S_1 state and the next excited state to a 3D_1 state.

5. Effect of low-mode truncation on the overlap factors

We now study the effect of removing the low-lying modes of the Dirac operator on the ratio a_V/a_T . Its effect on the hadron spectrum has been studied extensively, e.g. in Refs. [8, 9]. The Banks-Casher relation connects the low-lying modes of the Dirac operator to the quark condensate. Hence by removing the lowest eigenmodes we decouple our ρ states from the chiral symmetry breaking dynamics. The procedure of removing k lowest eigenmodes from the quark propagator is given by

$$D_k^{-1}(x,y) = D_{FULL}^{-1}(x,y) - \sum_{i=1}^k \frac{1}{\lambda_i} v_i(x) v_i^\dagger(y). \quad (5.1)$$

In Fig. 4 we show the value a_V/a_T for the ground state ρ and excited ρ' at different resolutions R for an increasing number of removed modes. For $k = 0$, i.e. the full theory, the mesons are a strong mixture of both chiral representations. With an increasing number of modes removed the ground state ρ meson approaches a pure $(0,1) \oplus (1,0)$ state, whereas the first excited state ρ' becomes a pure $(1/2, 1/2)_b$ state. Already at $k = 10$ the states are strongly dominated by one chiral representation: the chiral representations, which are slightly favored for $k = 0$, become dominant for $k \neq 0$.

In Fig. 2 it can be seen that after the removal of $\sim 10 - 20$ lowest modes both ρ and ρ' get degenerate and a $SU(4)$ symmetry [10, 11] of QCD in Euclidean space-time [12] becomes manifest. For other recent studies of this issue see Refs. [13, 14].

Acknowledgments

We thank the JLQCD collaboration for supplying us with the Overlap gauge configurations. We also thank M. Denissenya and C.B. Lang for discussions and help. The calculations have been performed on local clusters at ZID at the University of Graz and the Graz University of Technology. Support from the Austrian Science Fund (FWF) through the grants DK W1203-N16 and P26627-N27 is acknowledged.

References

- [1] K. A. Olive *et al.* [Particle Data Group Collaboration], *Chin. Phys. C* **38** (2014) 090001. doi:10.1088/1674-1137/38/9/090001
- [2] C. Rohrhofer, M. Pak and L. Y. Glozman, arXiv:1603.04665 [hep-lat].
- [3] L. Y. Glozman, C. B. Lang and M. Limmer, *Phys. Rev. Lett.* **103**, 121601 (2009) doi:10.1103/PhysRevLett.103.121601 [arXiv:0905.0811 [hep-lat]].
- [4] L. Y. Glozman, C. B. Lang and M. Limmer, *Phys. Lett. B* **705** (2011) 129 [arXiv:1106.1010 [hep-ph]].
- [5] L. Y. Glozman, C. B. Lang and M. Limmer, *Prog. Part. Nucl. Phys.* **67** (2012) 312 [arXiv:1111.2562 [hep-ph]].
- [6] L. Y. Glozman and A. V. Nefediev, *Phys. Rev. D* **76** (2007) 096004 [arXiv:0704.2673 [hep-ph]].
- [7] S. Aoki *et al.* [JLQCD Collaboration], *Phys. Rev. D* **78**, 014508 (2008).
- [8] M. Denissenya, L. Y. Glozman and C. B. Lang, *Phys. Rev. D* **89** (2014) 7, 077502 [arXiv:1402.1887 [hep-lat]].
- [9] M. Denissenya, L. Y. Glozman and M. Pak, *Phys. Rev. D* **92** (2015) 7, 074508 [*Phys. Rev. D* **92** (2015) 9, 099902] doi:10.1103/PhysRevD.92.099902, 10.1103/PhysRevD.92.074508 [arXiv:1508.01413 [hep-lat]].
- [10] L. Y. Glozman, *Eur. Phys. J. A* **51**, no. 3, 27 (2015) doi:10.1140/epja/i2015-15027-x [arXiv:1407.2798 [hep-ph]].
- [11] L. Y. Glozman and M. Pak, *Phys. Rev. D* **92**, no. 1, 016001 (2015) doi:10.1103/PhysRevD.92.016001 [arXiv:1504.02323 [hep-lat]].
- [12] L. Y. Glozman, arXiv:1511.05857 [hep-ph].
- [13] T. D. Cohen, *Phys. Rev. D* **93**, no. 3, 034508 (2016) doi:10.1103/PhysRevD.93.034508 [arXiv:1511.03956 [hep-lat]].
- [14] M. Shifman, *Phys. Rev. D* **93**, no. 7, 074035 (2016) doi:10.1103/PhysRevD.93.074035 [arXiv:1602.06699 [hep-ph]].